THE JOURNAL OF BIOLOGICAL CHEMISTRY Vol. 278, No. 22, Issue of May 30, pp. 20278–20285, 2003
Printed in U.S.A.

Covalent Trimers of the Internal N-terminal Trimeric Coiled-coil of gp41 and Antibodies Directed against Them Are Potent Inhibitors of HIV Envelope-mediated Cell Fusion*

Received for publication, February 14, 2003, and in revised form, March 24, 2003
Published, JBC Papers in Press, March 24, 2003, DOI 10.1074/jbc.M301627200

John M. Louis, Issa Nesheiwat, LengChee Chang, G. Marius Clore‡, and Carole A. Bewley§

From the Laboratories of Chemical Physics and Bioorganic Chemistry, NIDDK, National Institutes of Health, Bethesda, Maryland 20892

We have engineered two soluble, covalently linked, trimeric polypeptides, $N35_{CCG}$-N13 and $N34_{CCG}$ comprising only the internal trimeric coiled-coil of the ectodomain of HIV-1 gp41. Both trimers inhibit human immunodeficiency virus, type 1 (HIV-1) envelope (Env)-mediated cell fusion at nanomolar concentrations by targeting the exposed C-terminal region of the gp41 ectodomain in the prehairpin intermediate state. The IC_{50} values for $N35_{CCG}$-N13 and $N34_{CCG}$ are ~15 and ~95 nM, respectively, in a quantitative vaccinia virus-based reporter gene assay for HIV-1 Env-mediated cell fusion using Env from the T cell tropic strain LAV. Polyclonal antibodies were raised against $N35_{CCG}$-N13 and a tightly binding fraction of anti-$N35_{CCG}$-N13 inhibits T cell and macrophage tropic HIV-1 Env-mediated cell fusion with respective IC_{50} values of ~0.5 and ~1.5 μg/ml at 37 °C. The tightly binding anti-$N35_{CCG}$-N13 antibody fraction targets the exposed internal trimeric coiled-coil in the prehairpin intermediate state of gp41 in a manner analogous to peptides derived from the C region of the gp41 ectodomain. The potency of the tightly binding anti-$N35_{CCG}$-N13 antibody fraction in the fusion assay is comparable with that of the broadly neutralizing monoclonal antibody 2G12. These results indicate that $N35_{CCG}$-N13 is a potential anti-HIV therapeutic agent and represents a suitable immunogen for the generation of neutralizing monoclonal antibodies targeted to the internal trimeric coiled-coil of gp41. The data on the tightly binding anti-$N35_{CCG}$-N13 antibody fraction demonstrate that the internal trimeric coiled-coil of gp41 in the prehairpin intermediate state is accessible to antibodies and that access is not restricted by either antibody size or the presence of a kinetic barrier.

The first step in HIV[1] infection involves virus-cell or cell-cell fusion mediated by the viral envelope glycoproteins (Env) gp41 (transmembrane subunit of HIV envelope) and gp120 (surface envelope glycoprotein of HIV) (1). Both proteins therefore present highly attractive targets for the development of antiviral agents as well as broadly neutralizing antibodies. HIV Env-mediated cell fusion involves a complex series of events. gp120 first binds to CD4 and a chemokine receptor; this triggers conformational changes in the gp120-gp41 complex that lead to the insertion of the gp41 fusion peptide into the target membrane and ultimately to cell fusion (2, 3).

The structure of the ectodomain of gp41 (e-gp41) in its fusogenic/post-fusogenic state has been solved by both NMR (4) and crystallography (5–8) and consists of a trimer of hairpins comprising an internal parallel trimeric coiled-coil of N-terminal helices (residues 542–592 of HIV-1 Env (4)) surrounded by antiparallel C-terminal helices (residues 623–663 of HIV-1 Env (4)) (*left-hand side* of Fig. 1). The formation of the fusogenic/post-fusogenic state of e-gp41 provides the driving force for the apposition of the virus and cell membranes, thereby promoting membrane fusion (2). Prior to the formation of the fusogenic trimer of hairpins, e-gp41 exists in a "prehairpin" intermediate state (2, 9–12), so-called because the C region of e-gp41 (corresponding to the C-helices in the fusogenic/post-fusogenic state) is not yet associated with the internal trimeric coiled-coil of N-helices (Fig. 1, *middle*). In the prehairpin intermediate state both the internal trimeric coiled-coil (9, 10) and the C region of e-gp41 are accessible to inhibitors (13–15).

There are three classes of fusion inhibitors that target the prehairpin intermediate state of e-gp41 (*right-hand side* of Fig. 1). Class 1 inhibitors (shown in *blue* at the *top right* of Fig. 1) are directed against the internal trimeric coiled-coil of N-helices. Examples of class 1 inhibitors include peptides derived from the C-helices such as C34 (residues 628–661 of HIV-1 Env)[2] and T20 (also referred to as DP178, residues 638–673 of HIV-1 Env which extends 10 residues beyond the C-terminal end of the C-helix), both of which have IC_{50} values in the low nanomolar range (16–18). T20 is currently in the final stages of

* This work was supported by the Intramural AIDS Targeted Antiviral Program of the Office of the Director of the National Institutes of Health (to G. M. C. and C. A. B.). The costs of publication of this article were defrayed in part by the payment of page charges. This article must therefore be hereby marked "*advertisement*" in accordance with 18 U.S.C. Section 1734 solely to indicate this fact.

‡ To whom correspondence may be addressed: Laboratory of Chemical Physics, Bldg. 5, Rm. B1–30I, NIDDK, National Institutes of Health, Bethesda, MD 20892-0510. Tel.: 301-496-0782; Fax: 301-496-0825; E-mail: mariusc@intra.niddk.nih.gov.

§ To whom correspondence may be addressed: Laboratory of Bioorganic Chemistry, Bldg. 8, Rm. 1A-02, NIDDK, National Institutes of Health, Bethesda, MD 20892-0820. Tel.: 301-594-5187; E-mail: cb194k@nih.gov.

[1] The abbreviations used are: HIV, human immunodeficiency virus; Env, viral envelope glycoproteins; e-gp41, ectodomain of gp41; HPLC, high pressure liquid chromatography; PBS, phosphate-buffered saline; GnHCl, guanidine hydrochloride; Ni-NTA, nickel-nitrilotriacetic acid; Tricine, *N*-[2-hydroxy-1,1-bis(hydroxymethyl)ethyl]glycine; M tropic, macrophage tropic; T tropic, T cell line tropic.

[2] The nomenclature is as follows: N13, N34, N35, N36, C28, and C34 are peptides encompassing residues 546–558, 546–579, 546–580, 546–581, 628–655, and 628–661 of HIV-1 Env, respectively; $N34_{CCG}$ and $N35_{CCG}$ correspond to N34 and N35, respectively, with Leu^{576}, Gln^{577}, and Ala^{578} of HIV-1 Env substituted by Cys, Cys, and Gly, respectively; $N35_{CCG}$-N13 is a 48-residue peptide comprising $N35_{CCG}$ immediately followed by N13; N_{CCG}-gp41 is a chimeric protein comprising $N35_{CCG}$ fused onto the minimal thermostable ectodomain core of gp41: $N35_{CCG}$-N34-(L6)-C28, where L6 is a six-residue linker (SGGRGG); 6H, 20-residue non-native sequence derived from the cloning vector containing a His_6 tag.

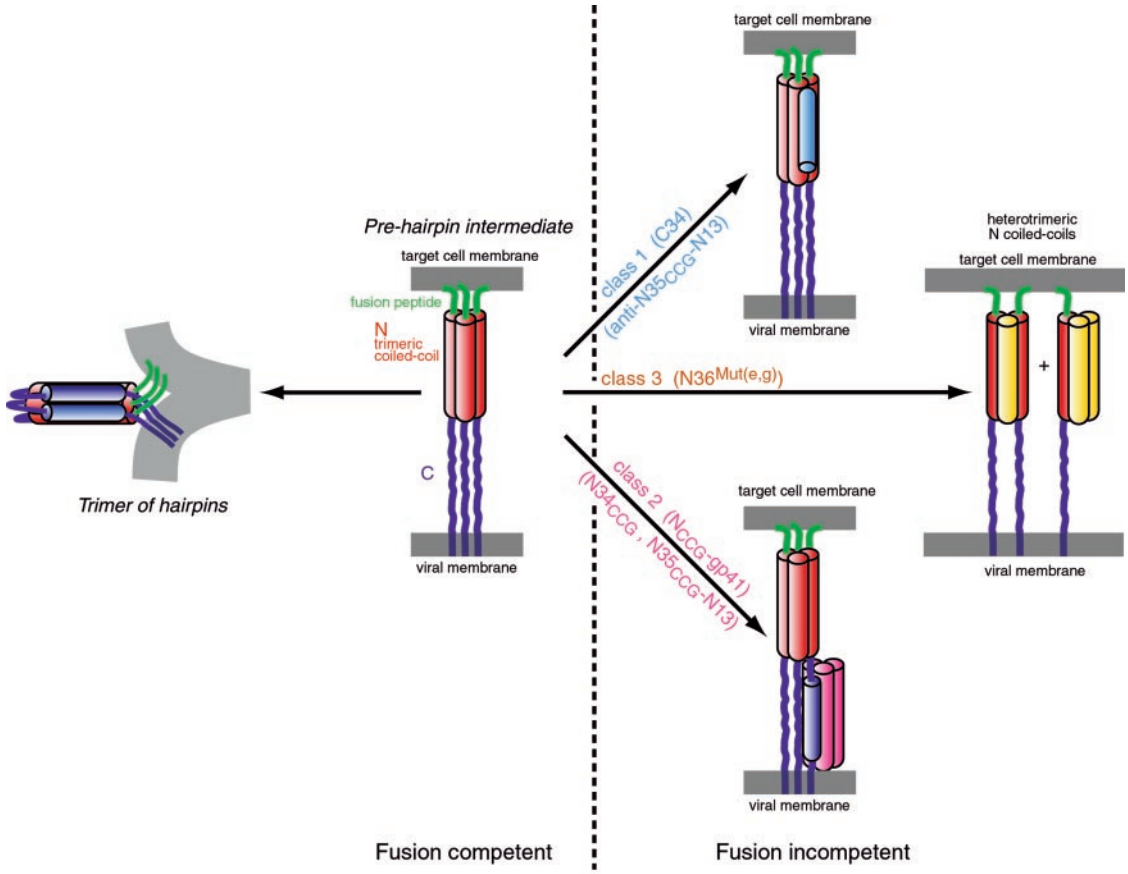

FIG. 1. **Inhibition of HIV-1 Env-mediated cell fusion by targeting the prehairpin intermediate state of gp41.** In the prehairpin intermediate state (shown in the *middle* of the figure), formed subsequent to the interaction of gp120 with CD4 and a chemokine receptor, the trimeric coiled-coil of N-helices (*red*) and the C-terminal region (*blue*) of the gp41 ectodomain are exposed. The prehairpin intermediate subsequently collapses to form a trimer of hairpins (whose structure has been solved by NMR (4) and crystallography (5–8)) bringing the target and viral membranes into apposition (*left-hand side* of figure). The N- and C-helices in the trimer of hairpins comprise residues 542–592 and 623–663, respectively, of HIV-1 Env (4). There are three classes of inhibitors (*right-hand side* of figure) that target the prehairpin intermediate and prevent its collapse into the trimer of hairpins, thereby rendering it fusion incompetent. Class 1 shown in *blue* (*e.g.* C34 (17) and the anti-$N35_{CCG}$-N13 antibodies described in the present paper) target the exposed trimeric coiled-coil of N-helices; class 2 shown in *red* (*e.g.* N_{CCG}-gp41 (13) and $N34_{CCG}$ and $N35_{CCG}$-N13 described in the present paper) target the C region; and class 3 shown in *yellow* (*e.g.* $N36^{Mut(e,g)}$ (22)) interact with the prehairpin intermediate state to form heterotrimers.

phase 3 clinical trials (19, 20). The class 2 inhibitors (shown in *red* at the *bottom right* of Fig. 1) are directed against the exposed C region of e-gp41. Examples include engineered proteins such as N_{CCG}-gp41 (13) and IQN17 (21), both of which expose the internal trimeric coiled-coil of e-gp41 in a stable manner, and the protein 5-helix, which exposes only a single helix of the internal trimeric coiled-coil (14). N_{CCG}-gp41, IQN17, and 5-helix have IC_{50} values in the 15–25 nM range. Finally, the class 3 inhibitors (shown in *yellow*, *middle right* of Fig. 1), exemplified by the construct $N36^{Mut(e,g)}$, which comprises a mutated version of the trimeric coiled-coil that can no longer interact with the C region of e-gp41, act by forming heterotrimers of the N-terminal coiled-coil (22).

The chimeric protein N_{CCG}-gp41 (Fig. 2) comprises an exposed trimeric coiled-coil of N-helices (residues 546–579 of HIV-1 Env with L576C, Q577C, and A578G mutations) that is stabilized by fusion to a minimal thermostable ectodomain of gp41 and by engineered intersubunit disulfide bonds (13). We anticipated that antibodies raised against N_{CCG}-gp41 could potentially target the exposed trimeric coiled-coil of N-helices in the prehairpin intermediate state of gp41 in a manner analogous to the class 1 inhibitors (13). However, antibodies directed against N_{CCG}-gp41 will inevitably comprise a mixture of antibodies that bind not only to the exposed trimeric coiled-coil of N-helices but also to the outer surface of the minimal thermostable ectodomain, which comprises the C-helices. To circumvent this problem, we have therefore engineered two simpler variants of N_{CCG}-gp41 that comprise only the internal trimeric coiled-coil of e-gp41: $N34_{CCG}$ and $N35_{CCG}$-N13 (Fig. 2). We show that these two variants are also nanomolar inhibitors of HIV-1 Env-mediated cell fusion. In addition, we demonstrate that purified anti-$N35_{CCG}$-N13-specific antibodies effectively inhibit HIV-1 Env-mediated cell fusion. The IC_{50} of the tight binding anti-$N35_{CCG}$-N13-specific antibody fraction is comparable with that of the broadly neutralizing, gp120 targeted, monoclonal antibody 2G12 (23, 24), which has just entered phase I clinical trials (25). These data indicate that the internal trimeric coiled-coil of e-gp41 is accessible to neutralizing antibodies in the prehairpin intermediate state and that $N35_{CCG}$-N13 represents a potentially suitable immunogen for the generation of therapeutic monoclonal antibodies.

EXPERIMENTAL PROCEDURES

Peptides—The C34 peptide (residues 628–661 of HIV-1 Env), purchased from Commonwealth Biotechnologies (Richmond, VA), was synthesized on a solid phase support, purified by reverse-phase high pressure liquid chromatography (HPLC), and verified for purity by mass spectrometry and amino acid analysis. C34 bears an acetyl group at the N terminus and an amide group at the C terminus.

Generation of $N34_{CCG}$ and $N35_{CCG}$-N13 Constructs—The synthesis and cloning of the chimeric protein N_{CCG}-gp41 (Fig. 2) has been described previously (13). N_{CCG}-gp41 comprises the engineered construct $N35_{CCG}$-N34-(L6)-C28, where $N35_{CCG}$ spans residues 546–580 of HIV-1 Env with L576C, Q577C, and A578G mutations, N34 spans residues

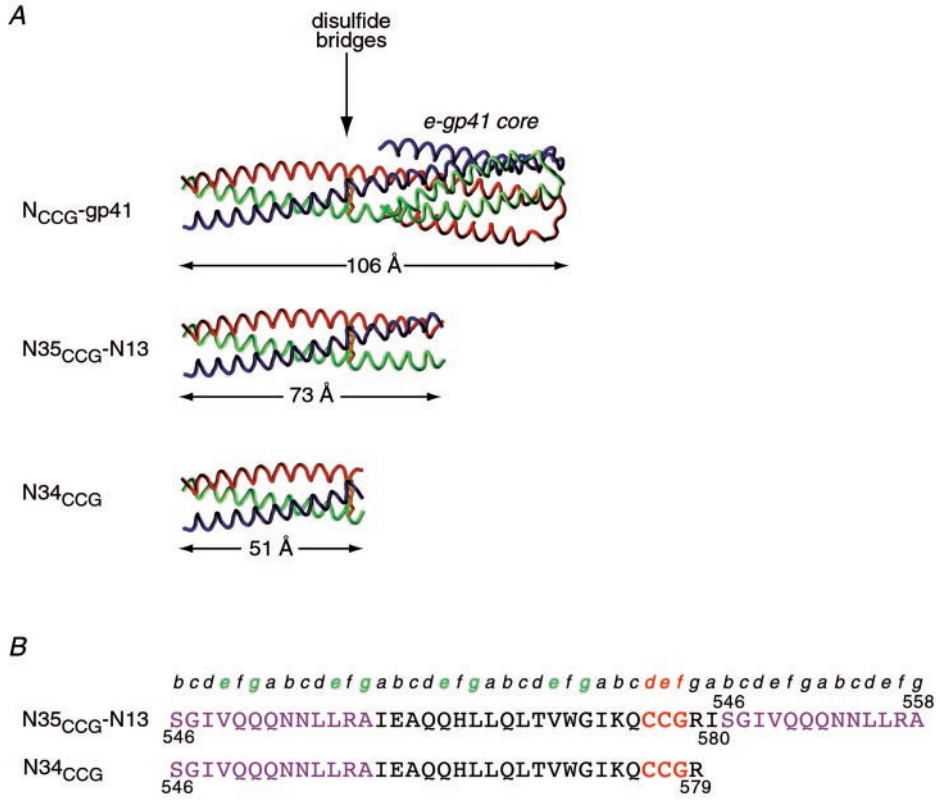

FIG. 2. **Design of N34$_{CCG}$ and N35$_{CCG}$-N13.** *A*, models of N$_{CCG}$-gp41 (13), N35$_{CCG}$-N13, and N34$_{CCG}$. The N34-(L6)-C28 gp41 core has been solved crystallographically (7). The model of N$_{CCG}$-gp41 was constructed by grafting N35 onto the N terminus of the crystal structure to generate a contiguous 69-residue helix comprising N35 and N34. The three intermolecular disulfide bridges formed by the two cysteines introduced at positions 576 and 577 are shown in *gold*, and the three subunits of the trimer are shown in *red*, *blue*, and *green*. The models of N35$_{CCG}$-N13 and N34$_{CCG}$ are directly derived from N$_{CCG}$-gp41. *B*, sequences of N35$_{CCG}$-N13 and N34$_{CCG}$. (Note that the expressed constructs of N35$_{CCG}$-N13 and N34$_{CCG}$ contain an additional 20-residue N-terminal region with a His$_6$ tag; see "Experimental Procedures.") The residue numbering is that of HIV-1 Env; the engineered Cys-Cys-Gly at positions 576–578 that have replaced the wild type Leu-Gln-Ala sequence are shown in *red*; N13 (residues 546–558 of HIV-1 Env) is indicated in *purple*; the *letters a–g* indicate the positions in a helical wheel presentation.

546–579 of HIV-1 Env, (L6) is a six-residue SGGRGG linker, and C28 spans residues 628–655 of HIV-1 Env. The insert spanning the N35$_{CCG}$-N34-(L6)-C28 domains was isolated by restriction digestion with *Nde*I and *Bam*HI enzymes, and cloned into the pET15b vector (Novagen, Madison, WI), which introduces an additional 20-residue, non-native segment (GSSHHHHHHSSGLVPRGSHM) at the N terminus containing a His$_6$ tag. The resulting construct 6H-N$_{CCG}$-gp41 was subsequently used to generate the N34$_{CCG}$ and N35$_{CCG}$-N13 constructs using the purified primers 5′-CTCACGGTCTGGGGCATCAAACAATGTTGTGGCCGCTAGTCCGGCATTGTGCAACAGCAAAACAACTTACTCGC and 5′-GTGCAACAGCAAAACAACTTACTGCGCGCGTAAGAAGCGCAGCAGCACCTGTTACATTG and their complements, respectively, together with the QuikChange mutagenesis protocol (Stratagene, La Jolla, CA). The N34$_{CCG}$ and N35$_{CCG}$-N13 constructs therefore also bear the 20-residue non-native His$_6$ tag at their N terminus. All constructs were verified by DNA sequencing and expressed in *Escherichia coli* BL21(DE3). The composition of all expressed proteins was confirmed by mass spectrometry. Note that N$_{CCG}$-gp41 was produced either with or without a His$_6$ linker and termed 6H-N$_{CCG}$-gp41 and N$_{CCG}$-gp41, respectively. N34$_{CCG}$ and N35$_{CCG}$-N13 were only produced with the His$_6$ tag linker sequence.

Purification and Protein Folding—The cells were grown at 37 °C in Luria-Bertani medium to an optical density of 0.7, induced with 2 mM isopropyl-β-D-thiogalactoside for 4 h, and harvested by centrifugation. The trimeric, intermolecular disulfide-linked form of N$_{CCG}$-gp41 was prepared exactly as described previously (13). To produce the trimeric, intermolecular disulfide-linked forms of the N34$_{CCG}$ and N35$_{CCG}$-N13, 2 gm of cells were suspended in 40 ml of 6 M guanidine hydrochloride (GnHCl), 50 mM Tris-HCl, pH 8.0, 1 mM β-mercaptoethanol (buffer A) and lysed by sonication, followed by centrifugation at 16,000 rpm (SS-34 rotor; Sorvall, Newtown, CT) for 30 min at 18 °C. The supernatant was subjected to Ni-NTA-agarose affinity column (bed volume, 10 ml) chromatography at room temperature. The column was washed in buffer A, and bound protein was eluted in the same buffer containing 0.2 M imidazole. The protein was concentrated on a Centriprep YM-3 device (Millipore Corporation, Bedford, MA) and applied at room temperature at a flow rate of 3 ml/min to a Superdex-75 column (HiLoad, 2.6 × 60 cm; Amersham Biosciences) equilibrated in 50 mM Tris-HCl, pH 8, 4 M GnHCl, 5 mM EDTA, and 5 mM dithiothreitol. The peak fractions were then subjected to reverse-phase HPLC on POROS 20 R2 resin (Applied Biosystems, Foster City, CA) using a linear gradient of 0–60% acetonitrile/0.05% trifluoroacetic acid. The peak fractions were pooled and stored at −80 °C.

~3.2 mg of C34 peptide (residues 628–661 of HIV-1 Env) was dissolved in 35% acetonitrile, 0.05% trifluoroacetic acid, H_2O containing ~2.2 mg of either N34$_{CCG}$ or N35$_{CCG}$-N13 protein at a concentration of 0.3 mg/ml. The polypeptide mixture (N34$_{CCG}$ + C34 or N35$_{CCG}$-N13 + C34), kept in a Slide-A-Lyzer cassette (3.5 molecular weight cutoff; Pierce), was folded by dialysis against 2 liters of 50 mM sodium formate buffer, pH 3.0, for 15 h at room temperature. The intermolecular disulfide bonds were then allowed to form by oxidation using the following dialysis scheme: 20 mM sodium phosphate, pH 6.25, for 2 h; 50 mM sodium formate, pH 3.0, for 3 h; 20 mM sodium phosphate, pH 4.25, for 15 h; and finally 50 mM sodium formate, pH 3.0, for 24 h. The N34$_{CCG}$/C34 and N35$_{CCG}$-N13/C34 complexes were concentrated to ~1 ml and analyzed by SDS-PAGE under nonreducing conditions to verify that N34$_{CCG}$ and N35$_{CCG}$-N13 were predominantly disulfide-linked trimers. The N34$_{CCG}$/C34 and N35$_{CCG}$-N13/C34 complexes were subsequently denatured in 7.5 M GnHCl, applied on a Superdex-75 column (2.6 × 60 cm; Amersham Biosciences) and fractionated under denaturing conditions in 4 M GnHCl, 50 mM sodium formate, pH 4. The peak fractions corresponding to the trimeric, disulfide-linked, N34$_{CCG}$ or N35$_{CCG}$-N13 proteins, stripped of C34, were pooled, dialyzed (3.5 MWCO; Pierce) against excess 50 mM sodium formate buffer, pH 3.0, concentrated (YM-3, Millipore), and stored at 4 °C.

Concentrations of all samples were determined spectrophotometrically; the calculated absorbances at 280 nm (1 cm path length) for a concentration of 1 mg/ml of N$_{CCG}$-gp41, N34$_{CCG}$, N35$_{CCG}$-N15, and C34 are 2.026, 0.987, 0.786, and 2.90, respectively. The corresponding molecular masses as monomers are 11863, 6011, 7546, and 4286 Da, respectively.

Circular Dichroism—CD spectra of $N34_{CCG}$ (10 μM) and $N35_{CCG}$-N15 (8 μM) were recorded in 20 mM sodium formate buffer, pH 3.0, at 25 °C on a JASCO J-720 spectropolarimeter using a 0.05-cm path length cell. Quantitative evaluation of secondary structure from the CD spectrum was carried out using the program CDNN (www.bioinformatik.biochemtech.uni-halle.de/cd_spect/index.html (26)).

Production of Antibodies and Purification of IgG—Antibodies to the intermolecular disulfide-linked 6H-$N34_{CCG}$ and 6H-$N35_{CCG}$-N13 trimers were raised in rabbits using the accelerated protocol services provided by Covance (Covance Research Products, Denver, PA) (27). 125 μg of $N34_{CCG}$ and 200 μg of $N35_{CCG}$-N13 was used for each initial and subsequent boost injections. Enzyme-linked immunosorbent assays to estimate antibody titers and IgG affinity purifications on immobilized protein A columns were performed according to established procedures (28). An average value of 1.7 absorbance units at 280 nm for 1 mg/ml was used to calculate the concentration of purified antibodies.

Western Blotting—Proteins, nonreduced and reduced (in the presence of β-mercaptoethanol), were subjected to SDS-PAGE on premade 10–20% linear gradient Tris-Tricine gels (Invitrogen). The gels were soaked for 10 min and then transferred onto a nitrocellulose membrane (Schleicher & Schuell) in 25 mM Tris buffer, pH 8, 190 mM glycine, and 20% methanol using a mini-electrophoretic transfer apparatus (Bio-Rad). The blots were then processed using a WesternBreeze kit, a chromogenic immunogenic system for the detection of rabbit primary antibodies (Invitrogen).

Purification of Anti-$N35_{CCG}$-N13-specific Antibodies—$N35_{CCG}$-N13 was bound to Ni-NTA-agarose via its N terminus His_6 tag as follows. 1.2–1.3 mg of $N35_{CCG}$-N13 in 15 ml of PBS, pH 6.5, was slowly dispensed into a beaker containing Ni-NTA-agarose (7.5 ml of packed volume) suspended and kept stirred in 15 ml of PBS, pH 6.5, at room temperature. The agarose was packed in a XK-26 column (Amersham Biosciences) and equilibrated in PBS, pH 6.5. 10 ml of protein A affinity chromatography-purified IgG (1.8 mg/ml) derived from rabbit antisera to $N35_{CCG}$-N13 was passed through the column at a flow rate of 0.5 ml/min. The unbound fraction was collected, and after washing the column extensively in PBS, the bound antibodies were eluted in 50 mM glycine, 0.15 M NaCl, pH 3.0. The peak fractions were immediately combined, and the pH was adjusted to 8.5 using 1 M Tris-HCl buffer, pH 9.0. The protein fraction that precipitates in the latter step was recovered by centrifugation at 3000 rpm for 15 min. The purification of antibodies from the pellet (precipitate) and supernatant (soluble) fractions was identical and conducted as follows. The pellet was solubilized and denatured in 10 ml of 6 M GnHCl, 50 mM Tris-HCl, pH 8.0. The supernatant was likewise denatured in 6 M GnHCl, 50 mM Tris-HCl, pH 8.0. The GnHCl-denatured material was passed through a fresh Ni-NTA-agarose column (packed volume, 7.5 ml) equilibrated in the same buffer. Refolding of IgG in the flow-through (~15 ml) was achieved by initial dialysis against 100-fold excess of 2 M GnHCl, 50 mM Tris-HCl, pH 8.0, buffer for about 5 h at room temperature, followed by extensive dialysis against PBS, pH 7.4, at 4 °C. The resulting two fractions of anti-$N35_{CCG}$-N13-specific IgG, one derived from the pellet, the other from the supernatant, were concentrated (YM-10; Pierce) and stored at −20 °C. As a control, protein A affinity-purified IgG from preimmune serum was also carried through the denaturation/refolding procedure.

Cell Fusion Assay—Inhibition of HIV Env-mediated cell fusion by $N34_{CCG}$, $N35_{CCG}$-N13, N_{CCG}-gp41, and the various antibodies was carried out as described previously (13) using a modification (29) of the vaccinia virus-based reporter gene assay employing soluble CD4. With the exception of recombinant vaccinia virus vCB-CCR5 (30), which was generously provided by Chris Broder, reagents were obtained from the National Institutes of Health AIDS Research and Reference Program, Division of AIDS, NIAID, National Institutes of Health as follows (contributors in parentheses): 2G12 monoclonal antibody (24) (Herman Katinger); vaccinia viruses vCB-32 (31), vCB-41 (31), and cVCYF1-fusin (32) (C. Broder, P. Kennedy, and E. Berger); and recombinant CD4 (Progenics Pharmaceuticals, Tarrytown, NY).

B-SC-1 cells were used for both target and effector cell populations. For experiments employing T-cell tropic Env, target cells were co-infected with recombinant vaccinia viruses vCB21R-LacZ (encoding β-galactosidase) and vCBYF1-fusin (encoding CXCR4) and effector cells with vCB41 (encoding Env from HIV-1 LAV) and vP11T7gene1 (encoding T7 polymerase) at a multiplicity of infection of 3.0. In the experiments employing macrophage (M) tropic Env, the target cells were co-infected with vCB-CCR5 (encoding the M tropic co-receptor CCR5) and vCB21R-LacZ and target cells with vCB21 (encoding Env from HIV-1 SF162) and vP11T7gene1. Following infection, the cells were incubated for 18 h at 32 °C to allow for vaccinia virus-mediated expression of recombinant proteins.

For inhibition studies, proteins or antibodies were added to an appropriate volume of 2.5% Dulbecco's modified Eagle's medium and PBS to yield identical buffer compositions (100 μl), followed by the addition of 1×10^5 effector cells (in 50 μl of medium)/well and 1×10^5 target cells (in 50 μl of medium)/well. Soluble CD4 was added to the medium of the target cells at a concentration of 800 nM to yield a final concentration of 200 nM soluble CD4/well. (This is double the concentration required to saturate the β-galactosidase signal; see Ref. 29). Following 2.5 h of incubation at 37 °C, the β-galactosidase activity of cell lysates was measured from the absorbance at 570 nm (Molecular Devices 96-well spectrophotometer) upon the addition of chorophenol red-β-D-galactopyranoside (Roche Applied Science). The curves for the percentage of fusion *versus* peptide inhibitor concentration were fit by nonlinear least squares optimization using the program Kaleidagraph 3.5 (Synergy Software, Reading, PA).

In terms of cytotoxicity, neither the trimeric proteins $N34_{CCG}$, $N35_{CCG}$-gp41, and N_{CCG}-gp41 nor the antibodies directed against $N35_{CCG}$-N13 showed any deleterious effects toward cell viability over the time period (2.5 h) of the fusion assay. We also note that previous experiments with our original N_{CCG}-gp41 construct (13) using an HIV-1 spreading assay in MT4 cells over a 25-day period indicated no evidence of cytotoxicity at a concentration of N_{CCG}-gp41 (400 nM) at which HIV-1 spreading (as measured by reverse transcriptase activity) was completely inhibited.[3]

RESULTS AND DISCUSSION

Rationale for the Design of $N34_{CCG}$ and $N35_{CCG}$-N13—We have previously shown that the chimeric protein N_{CCG}-gp41 (Fig. 2), which comprises an exposed, stable disulfide-linked, trimeric coiled-coil of N-helices grafted in helical phase onto the minimal thermostable core of e-gp41, inhibits HIV-1 Env-mediated cell fusion with an IC_{50} value of 15–20 nM. The N_{CCG}-gp41 construct is as follows: $N35_{CCG}$-N34-L6-C28 (see "Experimental Procedures"). The exposed, disulfide-linked, internal trimeric coiled-coil of e-gp41 is formed by $N35_{CCG}$, and the minimal thermostable core of e-gp41 is formed by N34-L6-C28.

From the perspective of a potential therapeutic, the N_{CCG}-gp41 trimer suffers from being rather large (~35 kDa). In terms of an immunogen, antibodies raised against N_{CCG}-gp41 will be targeted against two distinct epitopes: namely the exposed N-helical trimeric coiled-coil and the outer surface of the minimal e-gp41 core consisting of the C-helices. Thus, polyclonal antibodies raised against N_{CCG}-gp41 cannot be used to assess whether the internal trimeric coiled-coil represents a suitable target for neutralizing antibodies. We therefore sought to design smaller, covalently linked, soluble constructs consisting solely of the internal trimeric coiled-coil of e-gp41. To this end we engineered the two constructs $N34_{CCG}$ and $N35_{CCG}$-N13 (Fig. 2) by introducing stop codons at position Ile^{35} of the N35 portion and position Ile^{14} of the subsequent N34 portion, respectively, into the re-engineered 6H-N_{CCG}-gp41 construct having a His_6 tag at the N terminus (see "Experimental Procedures").

Preparation and Characterization of Disulfide-linked Trimers of the $N34_{CCG}$ and $N35_{CCG}$-N13 Analogs of the Internal Trimeric Coiled-coil of gp41—The chimeric protein N_{CCG}-gp41 folds spontaneously into a trimer, which becomes disulfide-linked upon air oxidation. In contrast, the same procedure applied to both $N34_{CCG}$ and $N35_{CCG}$-N13 yields trimers only to an extent of ~10%. More than 95% yield of disulfide-linked trimer of $N34_{CCG}$ and $N35_{CCG}$-N13, however, can readily be obtained in a three-step procedure: $N34_{CCG}$ and $N35_{CCG}$-N13 are first folded in the presence of C34 peptide (which comprises the C-helix region of the trimer of hairpins in the fusogenic/post-fusogenic state of e-gp41). This yields a trimer of the form $(N34_{CCG}/C34)_3$ (equivalent to the ectodomain core of fusogenic/post-fusogenic gp41) and $(N35_{CCG}\text{-}N13/C34)_3$, as evidenced by the elution profile of the complex at pH 3.0 on a Superdex-75

[3] R. Willey and M. A. Martin, personal communication.

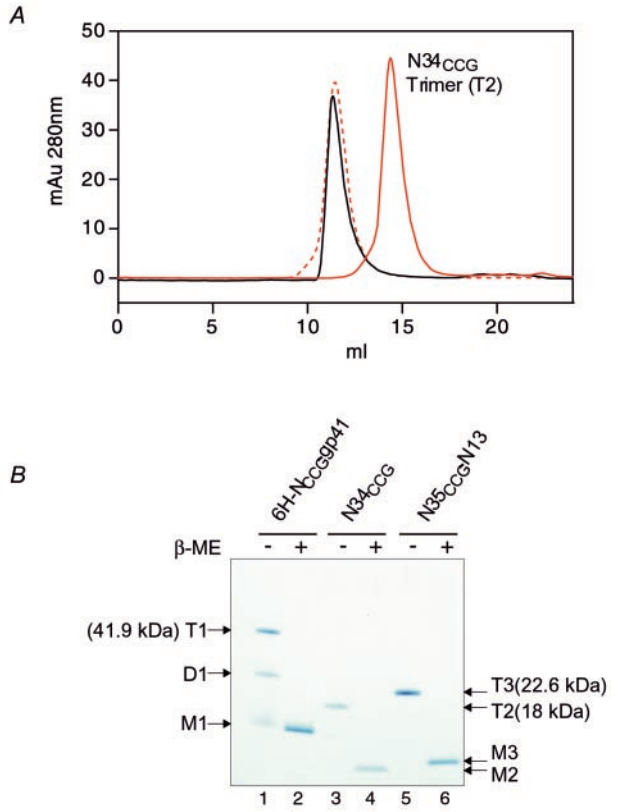

FIG. 3. **Biochemical characterization of $N34_{CCG}$ and $N35_{CCG}$-N13.** *A*, analysis of purified and folded trimeric N_{CCG}-gp41 (*black line*), $N34_{CCG}$ plus C34 peptide complex (*dashed red line*), and $N34_{CCG}$ (*red line*) by size exclusion column chromatography. The proteins were fractionated on a Superdex-75 column in 50 mM sodium formate buffer, pH 3.0, and 0.2 M GnHCl at room temperature. Note that the correct formation of disulfide-linked $N34_{CCG}$ trimer is promoted by association with the C34 peptide, which is subsequently stripped away as described in the text. *B*, SDS-PAGE analysis of N_{CCG}-gp41 (*lanes 1* and *2*), $N34_{CCG}$ (*lanes 3* and *4*), and $N35_{CCG}$-N13 (*lanes 5* and *6*). All samples were heated to 90 °C for 2 min. in the presence of 1.5% SDS in 50 mM Tris-HCl, pH 8.0, without (−) or with (+) β-mercaptoethanol, prior to loading on the gel. *T1*, *D1*, and *M1*, indicate the positions of the trimer, dimer, and monomer, respectively, of N_{CCG}-gp41; *T2* and *M2* indicate the positions of the trimer and monomer, respectively, of $N34_{CCG}$; and *T3* and *M3* the positions of the trimer and monomer, respectively of $N35_{CCG}$-N13.

column (Fig. 3*A*, profile shown by the *red dashed line* for $(N34_{CCG}/C34)_3$). This elution pattern is nearly the same as that for N_{CCG}-gp41, which only forms trimers (Fig. 3*A*, profile shown by the *black line*). Intermolecular disulfide bond formation between the three chains of $N34_{CCG}$ or $N35_{CCG}$-N13 in the $(N34_{CCG}/C34)_3$ or $(N35_{CCG}/N13\text{-}C34)_3$ complexes is then achieved by air oxidation, upon shifting the pH of the solution to 6.25. Finally, the $N34_{CCG}$ and $N35_{CCG}$-N13 disulfide-linked trimers are stripped from the C34 peptide by denaturation in 7.5 M GnHCl followed by size exclusion column chromatography (in 4 M GnHCl) and reverse-phase HPLC (see "Experimental Procedures"). Analysis of the purified folded trimeric form of $N34_{CCG}$ on a Superdex-75 column is shown by the *red trace* in Fig. 3*A*. SDS-polyacrylamide gel analysis of $N34_{CCG}$ and $N35_{CCG}$-N13 subsequent to folding by dialysis against 50 mM sodium formate buffer, pH 3, is shown in Fig. 3*B*. Both $N34_{CCG}$ and $N35_{CCG}$-N13 are completely trimeric under nonreducing conditions (Fig. 3*B*, *lanes 3* and *5*, bands labeled *T2* and *T3*, respectively). Treatment of the samples with a reducing agent prior to electrophoresis clearly results in both $N34_{CCG}$ and $N35_{CCG}$ migrating to the position of a monomer (Fig. 3*B*, *lanes 4* and *6*, labeled *M2* and *M3*, respectively).

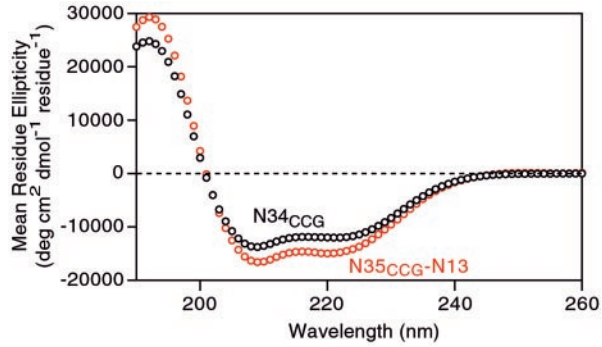

FIG. 4. **Characterization of disulfide-linked trimeric $N34_{CCG}$ and $N35_{CCG}$-N13 by CD spectroscopy.** CD spectra of the trimeric forms of $N34_{CCG}$ (10 μM) and $N35_{CCG}$-N13 (8 μM) were recorded in 20 mM sodium formate buffer, pH 3, at ambient temperature.

CD Spectra of Disulfide-linked Trimeric $N34_{CCG}$ and $N35_{CCG}$-N13—CD spectra of disulfide-linked trimeric $N34_{CCG}$ and $N35_{CCG}$-N13 are shown in Fig. 4. Both spectra display a double minimum at 208 and 222 nm, indicative of the presence of α-helix. Quantitative analysis of the spectra using the neural network program CDNN (26) yields an overall helical content of 43.0 ± 1.5% for $N34_{CCG}$ and 51.4 ± 0.9% for $N35_{CCG}$-N13. These values, however, also reflect the presence of the 20-residue His_6 tag at the N terminus that is expected to be random coil. Thus, the number of helical residues/subunit present in trimeric $N34_{CCG}$ and $N35_{CCG}$-N13 is 23.7 ± 0.8 and 35.5 ± 0.6, respectively. The difference in the number of helical residues between $N34_{CCG}$ and $N35_{CCG}$-N13 reflects the 14-residue extension of the trimeric coiled-coil in $N35_{CCG}$-N13. Assuming that the His_6 tag is random coil, these values yield percentage helicities within the e-gp41-derived regions of the $N34_{CCG}$ (34 residues) and $N35_{CCG}$-N13 (48 residues) constructs of 69.7 ± 2.4% for $N34_{CCG}$ and 74.0 ± 1.3% for $N35_{CCG}$-N13.

The CD data are therefore consistent with the models of $N34_{CCG}$ and $N35_{CCG}$-N13 displayed in Fig. 2*A*. The models, however, in Fig. 2*A* are depicted as fully helical. In reality, it is clear from the CD data that the N-terminal 9–10 residues of the e-gp41 derived regions of both constructs are likely to be frayed, and in the case of $N35_{CCG}$-N13, possibly the last 1–2 C-terminal residues as well.

$N34_{CCG}$ and $N35_{CCG}$-N13 Are Potent Inhibitors of HIV Env-mediated Cell Fusion—$N34_{CCG}$ and $N35_{CCG}$-N13 were tested in a quantitative vaccinia virus-based reporter gene assay to determine their effect on HIV-1 Env-mediated cell fusion (using Env from the T tropic HIV-1 strain LAV). The results are shown in Fig. 5. The IC_{50} values for $N34_{CCG}$ and $N35_{CCG}$-N13 are 96 ± 7 and 15.5 ± 1.3 nM, respectively. Also shown for comparison in Fig. 5 is the inhibition curve for N_{CCG}-gp41, which has an IC_{50} value of 19.3 ± 1.4 nM, consistent with previous data using the same fusion assay (13). (For reference, the IC_{50} for the C34 peptide, a potent class 1 inhibitor, under the same assay conditions is 2.3 ± 0.5 nM (13).) Thus, one can conclude that $N35_{CCG}$-N13 is equipotent with N_{CCG}-gp41, and the presence of the additional N13 segment coupled with the intermolecular disulfide bridge is sufficient to stabilize the appropriate region of the trimeric coiled-coil of N-helices in $N35_{CCG}$-N13. The 5–6-fold lower inhibitory activity of $N34_{CCG}$ relative to both $N35_{CCG}$-N13 and N_{CCG}-gp41 is presumably due to its slightly lower helical content, as a consequence of fraying at the N terminus.

Polyclonal Antibodies Specific to the Internal Trimeric Coiled-coil of gp41—Polyclonal antibodies to $N34_{CCG}$ and $N35_{CCG}$-N13 were raised in rabbits according to a standard protocol (27). The estimated 50% titers (*i.e.* the dilution at

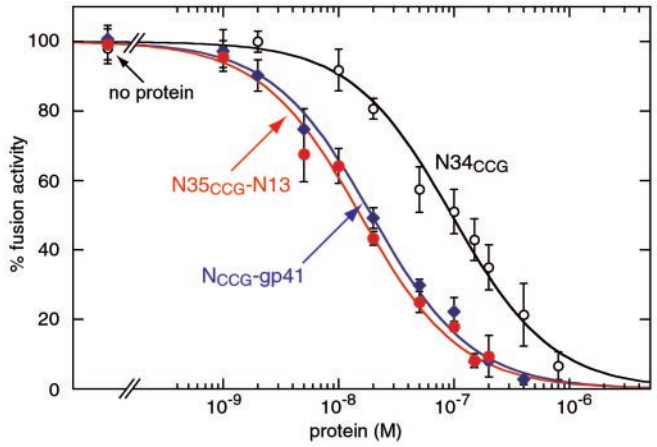

FIG. 5. **Inhibition of T tropic HIV-1 Env-mediated cell fusion by $N34_{CCG}$, $N35_{CCG}$-N13, and N_{CCG}-gp41 in a vaccinia virus-based reporter gene assay.** *Black open circles*, $N34_{CCG}$; *red solid circles*, $N35_{CCG}$-N13; *blue solid diamonds*, N_{CCG}-gp41. The *solid lines* represent best fits to the data using the simple activity relationship: percentage of fusion = $100/(1 + [I]/IC_{50})$, where [I] is the inhibitor concentration. The *vertical bars* indicate the standard deviations for the experimental data points. The calculated IC_{50} values for $N34_{CCG}$, $N35_{CCG}$-N13, and N_{CCG}-gp41 are 96 ± 7, 15.5 ± 1.3, and 19.3 ± 1.4 nM, respectively. HIV-Env is from the T tropic strain LAV of HIV-1, and the chemokine receptor is CXCR4.

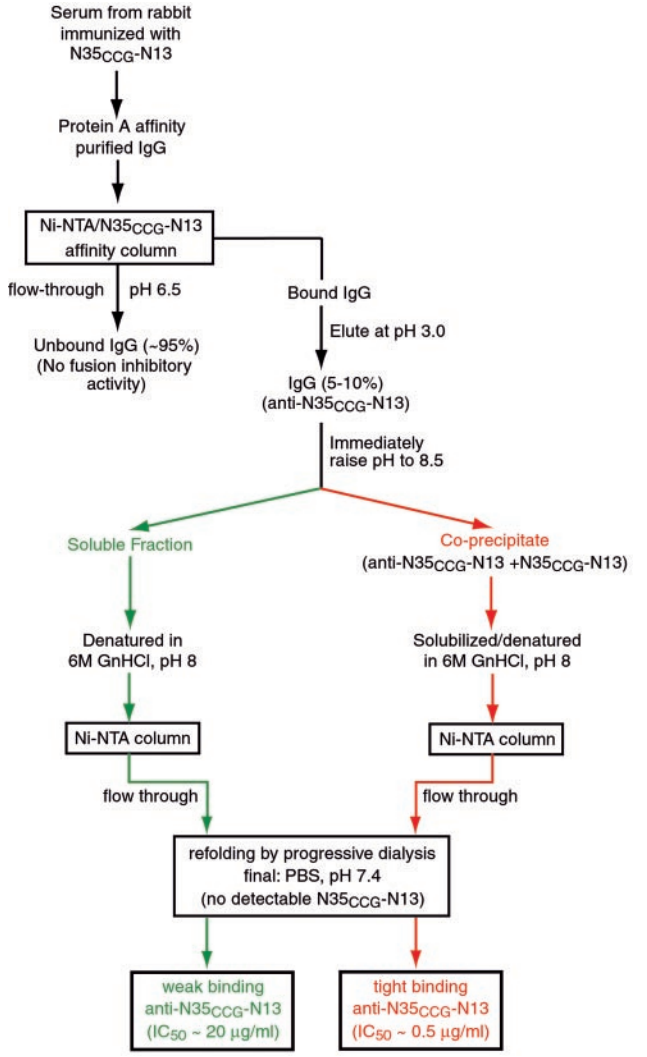

FIG. 6. **Scheme for the purification of anti-$N35_{CCG}$-N13-specific IgG.** Further details are provided under "Results and Discussion" and "Experimental Procedures." The partitioning of IgG in the co-precipitate (pellet) and soluble fractions obtained after elution from the Ni-NTA/$N35_{CCG}$-N13 column and raising the pH to 8.5 is approximately equal. Thus, the final yields of tight and weak binding anti-$N35_{CCG}$-N13 are about equal and correspond to ~2.5–5% of the total column input of the starting protein A-purified IgG under the conditions employed.

which 50% of antigen is bound using a concentration of 1 μg/ml of antigen) for antibodies directed against $N34_{CCG}$ and $N35_{CCG}$-N13 were 2.8×10^4 and 1.0×10^5, respectively, after 3–4 months. Sera from rabbits immunized with either $N34_{CCG}$ or $N35_{CCG}$-N13 reacted strongly with disulfide-linked N_{CCG}-gp41, $N34_{CCG}$, $N35_{CCG}$-N13 trimers on Western blots (data not shown), indicating that anti-$N34_{CCG}$ and anti-$N35_{CCG}$-N13 antibodies recognize the trimeric coiled-coil of N-helices. (Immunoblots using purified anti-$N35_{CCG}$-N13 antibodies are discussed below and displayed in Fig. 7*B*.) In contrast, the native N36 peptide (residues 546–581 of HIV-1 Env) reacts very poorly with the polyclonal antibodies (data not shown). N36, in the absence of C34, aggregates and does not form a unique species in solution (21, 22). This provides further evidence that the anti-$N34_{CCG}$ and anti-$N35_{CCG}$-N13 antibodies are targeted mainly to the folded trimeric coiled-coil of N-helices.

Because the 50% titer for the anti-$N35_{CCG}$-N13 serum was 3–4-fold higher than that for the anti-$N34_{CCG}$ serum, we chose to focus further purification on the anti-$N35_{CCG}$-N13 antibodies. The scheme employed is shown in Fig. 6 (see "Experimental Procedures" for details). Total IgG was first purified by protein A affinity chromatography (28). Fractions of the total IgG specific to the internal trimeric coiled-coil were then obtained by affinity chromatography using a $N35_{CCG}$-N13 immobilized Ni-NTA-agarose column. After elution of the unbound fraction (which comprises 90–95% of the total protein A purified IgG) and extensive washing with PBS, the IgG fraction bound to the immobilized $N35_{CCG}$-N13 was eluted at low pH (pH 3.0). At pH 3.0, elution of $N35_{CCG}$-N13 is also expected to occur because of protonation of the histidine residues in the His_6 tag, which therefore no longer bind nickel ions. Upon raising the pH of the peak fractions to 8.5, co-precipitation of a pool of tight binding anti-$N35_{CCG}$-N13-specific IgG and $N35_{CCG}$-N13 takes place, because of the poor solubility of $N35_{CCG}$-N13 at high pH. The distribution of IgG in the co-precipitate (pellet) and soluble (supernatant) fractions is approximately equal. The protein in the pellet fraction (harvested by centrifugation) was solubilized and denatured in 6 M GnHCl (33), passed through a column containing an excess of fresh Ni-NTA-agarose to completely remove any co-precipitated $N35_{CCG}$-N13, and refolded. IgG in the supernatant fraction was purified in exactly the same manner as the pellet fraction. The resulting purified tight (from the pellet) and weak (from the supernatant) anti-$N35_{CCG}$-N13-specific antibodies contain no residual $N35_{CCG}$-N13 as judged by SDS-PAGE (Fig. 7*A*) and mass spectrometry and react specifically with trimeric N_{CCG}-gp41, $N34_{CCG}$, and $N35_{CCG}$-N13 proteins observed by Western immunoblotting analysis (Fig. 7*B*). The absence of contaminating $N35_{CCG}$-N13 in the purified tight binding anti-$N35_{CCG}$-N13-specific IgG fraction was further confirmed by immunoblot analysis of the tight binding anti-$N35_{CCG}$-N13-specific IgG probed against itself (Fig. 7*C*).

Effect of Purified Anti-$N35_{CCG}$-N13-specific Antibodies on HIV-1 Env-mediated Cell Fusion—At 37 °C, serum from rabbits immunized against $N35_{CCG}$-N13 has no effect on HIV-1 Env mediated cell fusion in a vaccinia-virus based reporter gene assay. The purified tight binding anti-$N35_{CCG}$-N13-specific IgG, however, inhibits fusion completely at concentrations as low as 10 μg/ml; the weak binding anti-$N35_{CCG}$-N13-specific IgG inhibits fusion by ~90% at ~100 μg/ml. As a control, both protein A-purified preimmune IgG and preimmune IgG purified in exactly the same manner as that used for the anti-

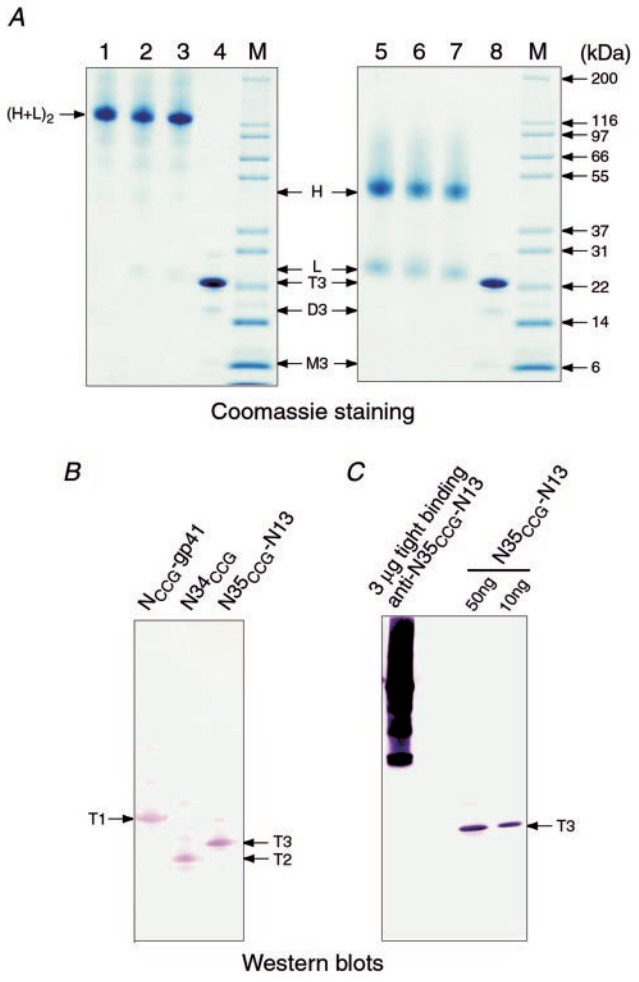

FIG. 7. **Characterization of anti-N35$_{CCG}$-N13 polyclonal antibodies.** *A*, SDS-PAGE of GnHCl denatured and refolded IgG (3.6 μg) on 10–20% Tris-Tricine precast gel (Invitrogen). *Lanes 1* and *5*, nonreduced and reduced (with β-mercaptoethanol), respectively, protein A affinity-purified IgG from preimmune serum. *Lanes 2* and *6*, nonreduced and reduced, respectively, weak binding anti-N35$_{CCG}$-N13-specific IgG (fraction indicated in *green* in the scheme shown in Fig. 6). *Lanes 3* and *7*, nonreduced and reduced tight binding anti-N35$_{CCG}$-N13-specific IgG (fraction indicated in *red* in the scheme shown in Fig. 6). *Lanes 4* and *8*, 2 μg of nonreduced N35$_{CCG}$-N13 protein. *Lane M*, molecular mass standard (Mark 12; Invitrogen). *(H+L)$_2$*, nonreduced IgG; *H*, heavy chain of IgG; *L*, light chain of IgG. *T3*, *D3*, and *M3* denote trimeric, dimeric, and monomeric N35$_{CCG}$-N13 protein, respectively. Densitometric scanning (National Institutes of Health Image version 1.6.1; rsb.info.nih.gov/nih-image) of the two N35$_{CCG}$-N13 lanes (*lanes 4* and *8*) indicate that the monomer M3 band represents ~3.3% of the total (T3+D3+M3) intensity, which corresponds to a protein quantity of ~65 ng. *B*, Western blot analysis of the N$_{CCG}$-gp41, N34$_{CCG}$, and N35$_{CCG}$-N13 proteins reacted with purified denatured/refolded tight binding anti-N35$_{CCG}$-N13-specific IgG (*i.e.* antibody shown in *lanes 3* and *7* of *panel A*) at a 1000-fold dilution from a 3.7 mg/ml stock solution. *T1*, *T2*, and *T3* denote the trimeric forms of N$_{CCG}$-gp41, N34$_{CCG}$, and N35$_{CCG}$-N13 proteins, respectively. *C*, a Western blot of overloaded purified tight binding anti-N35$_{CCG}$-N13-specific IgG (3 μg) probed against itself does not reveal the presence of any N35$_{CCG}$-N13 (*left-hand lane*). Control bands (*T3*) containing 50 and 10 ng of trimeric N35$_{CCG}$-N13 protein are also shown in the *middle* and *right lanes*, respectively. One can therefore conclude that the upper limit for any possible contaminating N35$_{CCG}$-N13 in the purified tight binding anti-N35$_{CCG}$-N13-specific antibody preparation is less than 0.5%. The samples were processed for SDS-PAGE as described in the Fig. 3 legend.

N35$_{CCG}$-N13-specific antibodies (*i.e.* including a GnHCl denaturation step followed by refolding) show no fusion inhibitory activity at a concentration of 100 μg/ml (Fig. 8). A quantitative comparison of the fusion inhibitory activity of the tight and weak binding anti-N35$_{CCG}$-N13-specific antibodies with that of

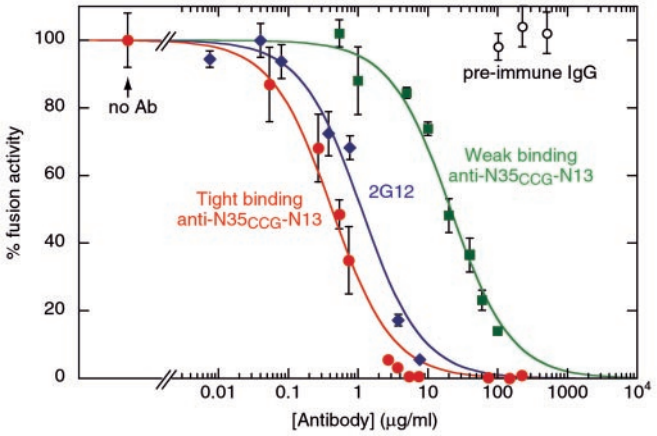

FIG. 8. **Inhibition of T tropic HIV-1 Env-mediated cell fusion by purified anti-N35$_{CCG}$-N13-specific antibodies in a vaccinia virus-based reporter gene assay.** *Red solid circles*, tight binding anti-N35$_{CCG}$-N13-specific IgG; *green solid squares*, weak binding anti-N35$_{CCG}$-N13-specific IgG; *blue solid diamonds*, 2G12 monoclonal antibody directed against gp120; *black open circles*, preimmune IgG. The *solid lines* represent best fits to the data using the simple activity relationship: percentage of fusion = 100/(1 + [I]/IC$_{50}$), where [I] is the inhibitor concentration. The *vertical bars* indicate standard deviations for the experimental data points. The calculated IC$_{50}$ values for strong binding anti-N35$_{CCG}$-N13, weak binding anti-N35$_{CCG}$-N13, and 2G12 are 0.42 ± 0.04 μg/ml, 21.2 ± 1.9 μg/ml, and 1.1 ± 0.2 μg/ml, respectively. The broadly neutralizing monoclonal antibody 2G12 is directed against an Asn-linked glycosylation site on gp120 (36, 37).

2G12, a broadly neutralizing monoclonal antibody directed against gp120 (23, 24), using Env from a T tropic strain of HIV-1 (LAV) is shown in Fig. 8. The apparent IC$_{50}$ values for the tight and weak binding anti-N35$_{CCG}$-N13-specific antibodies are ~0.4 and ~20 μg/ml, respectively, compared with ~1.5 μg/ml for 2G12. Cell fusion assays using an M tropic strain of HIV-1 were also carried out for the tight binding anti-N35$_{CCG}$-N13-specific antibodies and 2G12; inhibition of M tropic Env-mediated cell fusion by both antibodies is highly effective, although the IC$_{50}$ values are increased about 4-fold relative to those obtained with T tropic Env (Table I). These results therefore allow one to conclude that the tight binding anti-N35$_{CCG}$-N13-specific antibodies are highly potent inhibitors of HIV-1 fusion and are comparable in potency to the monoclonal antibody 2G12, which has just entered phase I clinical trials (25).

It is worth noting that antibodies raised against the native N36 peptide, which aggregates and does not form a helical trimeric coiled-coil (21, 22), do not inhibit HIV-1 Env-mediated cell fusion at 37 °C (34). However, these antibodies can inhibit fusion if the target and effector cells are incubated for 1–2 h at a reduced temperature (31.5 °C) to prolong the lifetime of fusion intermediates prior to initiating fusion by raising the temperature to 37 °C (35). These data suggested the presence of a kinetic barrier hindering access of antibodies to the internal trimeric coiled-coil in the prehairpin intermediate state (35). The current data with the purified anti-N35$_{CCG}$-N13-specific antibodies indicate that no such kinetic barrier exists, and the much higher degree of potency of the tight binding anti-N35$_{CCG}$-N13-specific antibodies can be attributed to their very high avidity for the folded internal trimeric coiled-coil.

Concluding Remarks—Using rational design we have engineered two soluble, covalently linked, trimeric polypeptides (N34$_{CCG}$ and N35$_{CCG}$-N13) comprising only the internal trimeric coiled-coil of e-gp41. Both constructs inhibit HIV-1 Env-mediated cell fusion at nanomolar concentrations, and N35$_{CCG}$-N13 has the same potency as the previously engineered chimeric protein N$_{CCG}$-gp41, which comprises the internal tri-

TABLE I

Comparison of inhibition of T tropic (LAV) and M tropic (SF162) HIV-1 Env-mediated cell fusion in the vaccinia virus-based reporter gene assay by the tightly binding anti-$N35_{CCG}$-N13-specific antibody fraction and the 2G12 monoclonal antibody (directed against gp120)

The remote possibility that the fusion inhibitory activity of the anti-$N35_{CCG}$-N13-specific antibodies could be due to the presence of any contaminating $N35_{CCG}$-N13 is completely excluded by the data in Fig. 7C, which place an upper limit of less than 0.5% for the percentage of any $N35_{CCG}$-N13 present in the denatured/refolded purified anti-$N35_{CCG}$-N13-specific IgG preparations. The IC_{50} of $N35_{CCG}$-N13 is ≈16 nM (Fig. 5), which corresponds to a concentration of ≈0.4 μg/ml; thus, at concentrations of tight binding anti-$N35_{CCG}$-N13-specific antibody corresponding to the IC_{50} values for inhibition of T tropic and M tropic Env-mediated cell fusion, the maximum upper limit of any contaminating $N35_{CCG}$-N13 is <2 and <7.5 ng/ml, respectively; at such low concentrations $N35_{CCG}$-N13 displays no fusion inhibitory activity.

	IC_{50}	
	T tropic	M tropic
	μg/ml	
Tightly binding anti-$N35_{CCG}$-N13	0.42 ± 0.04	1.5 ± 0.3
2G12	1.1 ± 0.2	4.4 ± 1.8

meric coiled-coil grafted onto the minimal thermostable core of e-gp41. The much smaller size of $N35_{CCG}$-N13 makes it a potentially useful therapeutic agent in its own right.

Antibodies raised against $N35_{CCG}$-N13 are specifically targeted to the folded internal trimeric coiled-coil and therefore have the potential to inhibit fusion in a manner analogous to the class 1 inhibitors derived from the C-helical region of e-gp41 (Fig. 1). Although total sera from rabbits immunized with $N35_{CCG}$-N13 do not inhibit fusion, a very potent fusion inhibitory fraction, comprising 2.5–5% of the total IgG, can be readily purified by affinity chromatography on a $N35_{CCG}$-N13 immobilized column. The tight binding anti-$N35_{CCG}$-N13-specific antibody fraction inhibits both T tropic and M tropic HIV-1 Env-mediated cell fusion at 37 °C and, in a vaccinia virus-based reporter gene assay, is comparable in potency to the broadly neutralizing monoclonal antibody 2G12 directed against gp120. These results therefore indicate that the internal trimeric coiled-coil of e-gp41 is accessible to antibodies in the prehairpin intermediate state and that access is not limited by a kinetic barrier. Thus, although $N35_{CCG}$-N13 in its present state does not appear to be suitable as a vaccine, $N35_{CCG}$-N13 represents a potentially suitable immunogen for the generation of therapeutic monoclonal antibodies. In terms of an effective vaccine, it is clear that the fraction in immunized serum of tight binding antibodies directed toward the internal trimeric coiled-coil of e-gp41 needs to be dramatically increased. This could potentially be achieved by engineering multivalent versions of $N35_{CCG}$-N13.

Acknowledgments—We thank Chris Broder for an aliquot of the recombinant vaccinia virus vCB-CCR5; Satyajit Ray and Shannon Lynch for expert technical assistance; Carol Weiss for helpful discussions; and Malcom Martin and Ron Willey for communicating results of an HIV-1 spreading assay on N_{CCG}-gp41. All other recombinant viruses, 2G12, and soluble two-domain CD4 were obtained from the National Institutes of Health AIDS Research and Reference Reagent Program (Rockville, MD; www.aidsreagent.org).

REFERENCES

1. Freed, E. O., and Martin, M. A. (1995) *J. Biol. Chem.* **270,** 23883–23886
2. Moore, J. P., Trkola, A., and Dragic, T. (1997) *Curr. Opin. Immunol.* **9,** 551–562
3. Eckert, D. M., and Kim, P. S. (2001) *Annu. Rev. Biochem.* **70,** 777–810
4. Caffrey, M., Cai, M., Kaufman, J., Stahl, S. J., Wingfield, P. T., Covell, D. G., Gronenborn, A. M., and Clore, G. M. (1998) *EMBO J.* **17,** 4572–4584
5. Chan, D. C., Fass, D., Berger, J. M., and Kim, P. S. (1997) *Cell* **89,** 263–273
6. Weissenhorn, W., Dessen, A., Harrison, S. C., Skehel, J. J., and Wiley, D. C. (1997) *Nature* **387,** 426–430
7. Tan, K. J., Liu, J., Wang, S., Shen, S., and Lu, M. (1997) *Proc. Natl. Acad. Sci. U. S. A.* **94,** 12303–12308
8. Malashkevich, V. N., Chan, D. C., Chutkowski, C. T., and Kim, P. S. (1998) *Proc. Natl. Acad. Sci. U. S. A.* **95,** 9134–9139
9. Furuta, R. A., Wild, C. T., Weng, Y., and Weiss, C. D. (1998) *Nat. Struct. Biol.* **5,** 276–279
10. Chan, D. C., and Kim, P. S. (1998) *Cell* **93,** 681–684
11. Muñoz-Barroso, I., Durell, S., Sakaguchi, K., Appella, E., and Blumenthal, R. (1998) *J. Cell Biol.* **140,** 315–323
12. Kliger, Y., Gallo, S. A., Peisajovich, S. G., Munoz-Barraso, I., Avkin, S., Blumenthal, R., and Shai, Y. (2001) *J. Biol. Chem.* **276,** 1391–1397
13. Louis, J. M., Bewley, C. A., and Clore, G. M. (2001) *J. Biol. Chem.* **276,** 29485–29489
14. Root, M. J., Kay, M. S., and Kim, P. S. (2001) *Science* **291,** 884–888
15. Koshiba, T., and Chan, D. C. (2003) *J. Biol. Chem.* **278,** 7573–7579
16. Wild, C. T., Shugars, D. C., Greenwell, T. K., McDanal, C. B., and Matthews, T. J. (1994) *Proc. Natl. Acad. Sci. U. S. A.* **91,** 9770–9774
17. Chan, D. C., Chutkowski, C. T., and Kim, P. S. (1998) *Proc. Natl. Acad. Sci. U. S. A.* **95,** 15613–15617
18. Kliger, Y., and Shai, Y. (2000) *J. Mol. Biol.* **295,** 163–168
19. Kilby, J. M., Hopkins, S., Venetta, T. M., DiMassimo, B., Cloud, G. A., Lee, J. Y., Alldredge, L., Hunter, E., Lambert, D., Bolognesi, D., Matthews, T., Johnson, M. R., Nowak, M. A., Shaw, G. M., and Saag, M. S. (1998) *Nat. Med.* **4,** 1302–1307
20. Kilby, J. M., Lalezari, J. P., Eron, J. J., Carson, M., Cohen, C., Arduino, R. C., Goodgame, J. C., Gallant, J. E., Volberding, P., Murphy, R. L., Valentine, F., Saag, M. S., Nelson, E. L., Sista, P. R., and Dusek, A. (2002) *AIDS Res. Hum. Retroviruses* **18,** 685–693
21. Eckert, D. M., and Kim, P. S. (2001) *Proc. Natl. Acad. Sci. U. S. A.* **98,** 11187–11192
22. Bewley, C. A., Louis, J. M., Ghirlando, R., and Clore, G. M. (2002) *J. Biol. Chem.* **277,** 14238–14245
23. Trkola, A, Pomals, A. P., Yuan, H., Korber, B., Maddon, J., Allaway, G., Katinger, H., Barbas, C. F., III Burton, D. R., Ho, D., and Moore, J. P. (1995) *J. Virol.* **69,** 6609–6617
24. Trkola, A., Purtscher, M., Muster, T., Ballaun, C., Buchacher, A., Sullivan, N., Srinivasan, K., Sodroski, J., Moore, J. P., and Katinger, H. (1996) *J. Virol.* **70,** 1100–1108
25. Stiegler, G., Armbuster, C., Vcelar, B., Stoiber, H., Kunert, R., Michael, N. L., Jagodzinski, L. L., Ammann, C., Jager, W., Jacobson, J., Veller, N., and Kattinger, H. (2002) *AIDS* **16,** 2019–2025
26. Bohm, G., Muhr, R., and Jaenicke, R. (1992) *Protein Eng.* **5,** 191–195
27. Vaitukaitis, J. L. (1981) *Methods Enzymol.* **73,** 46–52
28. Harlow, E., and Lane, D. (1988) *Antibodies: A Laboratory Manual*, Cold Spring Harbor Laboratory, Cold Spring Harbor, NY
29. Salzwedel, K., Smith, E., Dey, B., and Berger, E. A. (2000) *J. Virol.* **74,** 326–333
30. Dimitrov, D. S., Norwood, D., Stantchev, R. S., Feng, Y., Xiao, S., and Broder, C. C. (1999) *Virology* **259,** 1–6
31. Broder, C. C., and Berger, E. A. (1995) *Proc. Natl. Acad. Sci. U. S. A.* **92,** 9004–9008
32. Feng, Y., Broder, C. C., Kennedy, P. E., and Berger, E. A. (1996) *Science* **272,** 872–877
33. Nashi, L. O., Caughey, D. J., Horan, T. P., Kita, Y., Chand, D., and Arakawa, T. (1997) *Anal. Biochem.* **253,** 246–252
34. de Rosny, E., Vassell, V., Wingfield, P. T., Wild, C. T., and Weiss, C. D. (2001) *J. Virol.* **75,** 8859–8863
35. Golding, H., Zaitseva, M., de Rosny, E., King, L. R., Maischewitz, J., Sidorow, I., Gorny, M. K., Zolla-Pazner, S., Dimitrov, D. S., and Weiss, C. D. (2002) *J. Virol.* **76,** 6780–6790
36. Sanders, R. W., Venturi, M., Schiffner, L., Kalyanaraman, R., Katinger, H., Lloyd, K. O., Kwong, P, D., and Moore, J. P. (2002) *J. Virol.*, **76,** 7293–7305
37. Scanlon, C. N., Pantophlet, R., Wormlad, M. R., Saphire, E. O., Stanfield, R., Wilson, I. A., Katinger, H., Dwek, R. A., Rudd, P. M., and Burton, D. R. (2002) *J. Virol.* **76,** 7306–7321